

A Model for Visual Camouflage Breaking

Ariel Tankus* and Yehezkel Yeshurun*

Department of Computer Science
Tel-Aviv University
Tel-Aviv 69978, Israel
{arielt, hezy}@math.tau.ac.il

Abstract. Some animals use counter-shading in order to prevent their detection by predators. Counter-shading means that the albedo of the animal is such that its image has a flat intensity function rather than a convex intensity function. This implies that there might exist predators who can detect 3D objects based on the convexity of the intensity function. In this paper, we suggest a mathematical model which describes a possible explanation of this detection ability. We demonstrate the effectiveness of convexity based camouflage breaking using an operator (“ D_{arg} ”) for detection of 3D convex or concave graylevels. Its high robustness and the biological motivation make D_{arg} particularly suitable for camouflage breaking. As will be demonstrated, the operator is able to break very strong camouflage, which might delude even human viewers. Being non-edge-based, the performance of the operator is juxtaposed with that of a representative edge-based operator in the task of camouflage breaking. Better performance is achieved by D_{arg} for both animal and military camouflage breaking.

1 Introduction

“Camouflage is an attempt to obscure the signature of a target and also to match its background” [1]. Work related to camouflage can be roughly divided into two: camouflage assessment and design (e.g, [1], [2]), and camouflage breaking. Despite the ongoing research, only little has been said in the computer vision literature on visual camouflage breaking: [6], [11], [5], [3], [4]

In this paper, we address the issue of *visual camouflage breaking*. We present biological evidence that detection of the convexity of the graylevel function may be used to break camouflage. This is based on Thayer’s principle of counter-shading [12], which observes that some animals use apatetic coloration to prevent their image (under sun light) from appearing as convex graylevels to a viewer. This implies that other animals may break camouflage based on the convexity of the graylevels they see (or else there was no need in such an apatetic coloration).

Our goal is therefore to detect 3D convex or concave objects under strong camouflage. For this task, we employ our proposed operator (D_{arg}), which is applied directly to the intensity function. D_{arg} responds to smooth 3D convex or concave patches in objects. The operator is not limited by any particular light source or reflectance function.

* Supported by the Minerva Minkowski center for geometry, and by grant from the Israel Academy of Science for Geometric Computing.

It does not attempt to restore the three dimensional scene. The purpose of the operator is *detection* of convex or concave objects in highly cluttered scenes, and in particular under camouflage conditions.

The robustness and invariance characterizing D_{arg} (see [10]) as well as the biological motivation make it suitable for camouflage breaking, even for camouflages that might delude a human viewer. In contrast with existing attempts to break camouflage, our operator is context-free; its only a priori assumption about the target is its being three dimensional and convex (or concave). In order to evaluate the performance of the operator in breaking camouflage, we juxtaposed D_{arg} with a representative edge-based operator. Due to lack of room only a small portion of the comparison can be given in the paper.

The next section defines the operator D_{arg} for convexity-based detection. Section 2.1 gives intuition for D_{arg} and is of particular importance for understanding its behavior. Section 3 utilizes D_{arg} for camouflage breaking. Section 3.1 brings the biological evidence for camouflage breaking by detection of graylevel convexity. Section 3.2 establishes the connection between the biological evidence and the specific convexity detector D_{arg} . Section 4 delineates a camouflage breaking comparison of an edge-based method with our convexity detector. Concluding remarks are in section 5.

2 Y_{arg}, D_{arg} : Operators for Detection of Convex Domains

We next define an operator for detection of three dimensional objects with smooth convex and concave domains.

Let $I(x, y)$ be an input image, and $\nabla I(x, y) = (\frac{\partial}{\partial x}I(x, y), \frac{\partial}{\partial y}I(x, y))$ the Cartesian representation of the gradient map of $I(x, y)$. Let us convert $\nabla I(x, y)$ into its *polar* representation. The gradient argument is defined by:

$$\theta(x, y) = \arg(\nabla I(x, y)) = \arctan \left(\frac{\partial}{\partial y}I(x, y) , \frac{\partial}{\partial x}I(x, y) \right)$$

where the two dimensional arc tangent is:

$$\arctan(y, x) = \begin{cases} \arctan(\frac{y}{x}), & \text{if } x \geq 0 \\ \arctan(\frac{y}{x}) + \pi, & \text{if } x < 0, y \geq 0 \\ \arctan(\frac{y}{x}) - \pi, & \text{if } x < 0, y < 0 \end{cases}$$

and the one dimensional $\arctan(t)$ denotes the inverse function of $\tan(t)$ so that: $\arctan(t) : [-\infty, \infty] \mapsto [-\frac{\pi}{2}, \frac{\pi}{2}]$.

The proposed convexity detection mechanism, which we denote: Y_{arg} , is simply the y -derivative of the argument map:

$$Y_{arg} = \frac{\partial}{\partial y}\theta(x, y) = \frac{\partial}{\partial y} \arctan \left(\frac{\partial}{\partial y}I(x, y) , \frac{\partial}{\partial x}I(x, y) \right)$$

To obtain an isotropic operator based on Y_{arg} , we rotate the original image by 0° , 90° , 180° and 270° , operate Y_{arg} , and rotate the results back to their original positions. The sum of the four responses is the response of an operator which we name: D_{arg} .

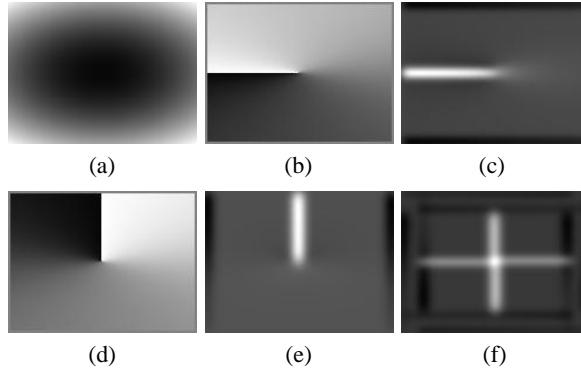


Fig. 1. (a) Paraboloidal gray-levels: $I(x, y) = 100x^2 + 300y^2$. (b) Gradient argument of (a). Discontinuity ray at the negative x -axis. (c) Y_{arg} of (a) ($= \frac{\partial}{\partial y}$ of (b)). (d) Rotation of (a) (90° c.c.w.), calculation of gradient argument, and inverse rotation. (e) Rotation of (a) (90° c.c.w.), calculation of Y_{arg} , and inverse rotation. (f) Response of D_{arg} , the isotropic operator.

2.1 Intuitive Description of the Operator

– What Does Y_{arg} Detect?

Y_{arg} detects the zero-crossings of the gradient argument. This stems from the last step of the gradient argument calculation: the two-dimensional arc-tangent function. The arc-tangent function is discontinuous at the negative part of the x -axis; therefore its y -derivative approaches infinity there. In other words, Y_{arg} approaches infinity at the negative part of the x -axis of the arctan, when this axis is being crossed. This limit reveals the zero-crossings of the gradient argument (see [10] for more details).

– Why Detect Zero-Crossings of the Gradient Argument?

Y_{arg} detects zero-crossings of the gradient argument of the intensity function $I(x, y)$. The existence of zero-crossings of the gradient argument enforces a certain range of values on the gradient argument (trivially, values near zero). Considering the intensity function $I(x, y)$ as a surface in \mathbb{R}^3 , the gradient argument “represents” the direction of the normal to the surface. Therefore, a range of values of the gradient argument means a certain range of directions of the normal to the intensity surface. This enforces a certain structure on the intensity surface itself.

In [10] we have characterized the structure of the intensity surface as either a paraboloidal structure or any derivable strongly monotonically increasing transformation of a paraboloidal structure (Fig. 1). Since paraboloids are arbitrarily curved surfaces, they can be used as a local approximation of 3D convex or concave surfaces (Recall, that our input is discrete, and the continuous functions are only an approximation!). The detected intensity surface patches are therefore those exhibiting 3D convex or concave structure. The convexity is three dimensional, because this is the convexity of the intensity surface $I(x, y)$ ($= 2D$ surface in \mathbb{R}^3 ; Fig. 2(b)), and *not* convexity of contours ($= 1D$ surface in \mathbb{R}^2 ; Fig. 2(a)). This 3D convexity of the intensity surface is characteristic of intensity surfaces emanating from smooth 3D convex bodies.

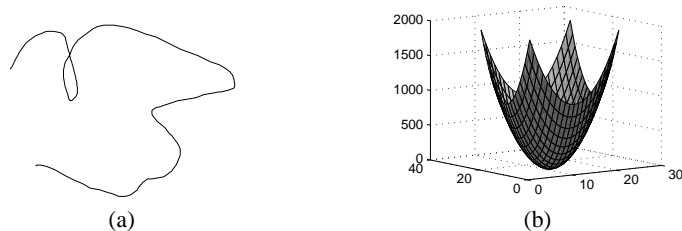


Fig. 2. 3D vs. 2D convexity. (a) 2D convexity: A contour is a 1D surface in \mathbb{R}^2 . (b) 3D convexity: A paraboloid is a 2D surface in \mathbb{R}^3 .

– Summary

We detect the zero-crossings of the gradient argument by detecting the infinite response of Y_{arg} at the negative x -axis (of the arctan). These zero-crossings occur where the intensity surface is 3D convex or concave. Convex smooth 3D objects usually produce 3D convex intensity surfaces. Thus, detection of the infinite responses of Y_{arg} results in detection of domains of the intensity surface which characterize 3D smooth convex or concave subjects.

3 Camouflage Breaking

The robustness of the operator under various conditions (illumination, scale, orientation, texture) has been thoroughly studied in [10]. As a result, the smoothness condition of the detected 3D convex objects can be relaxed. In this paper, we further increase the robustness demands from the operator by introducing very strong camouflage.

3.1 Biological Evidence for Camouflage Breaking by Convexity Detection

Next, we exhibit evidence of biological camouflage breaking based on detection of the convexity of the intensity function. This matches our idea of camouflage breaking by direct convexity estimation (using D_{arg}). We bring further evidence, that not only can intensity convexity be used to break camouflage, but also there are animals whose coloring is suited to prevent this specific kind of camouflage breaking.

It is well known that under directional light, a smooth three dimensional convex object produces a convex intensity function. The biological meaning is that when the trunk of an animal (the convex subject) is exposed to top lighting (sun), a viewer sees shades (convex intensity function). As we shall see, these shades may reveal the animal, especially in surroundings which break up shadows (e.g., woods) (see [8]). This biological evidence supports D_{arg} approach of camouflage breaking by detecting the convexity of the intensity function.

The ability to trace an animal based on these shadow effects has led, during thousands of years of evolution, to coloration of animals that dissolves the shadow effects. This counter-shading coloration was first observed at the beginning of the century [12], and is known as Thayer's principle. Portmann [8] describes Thayer's principle: "If we

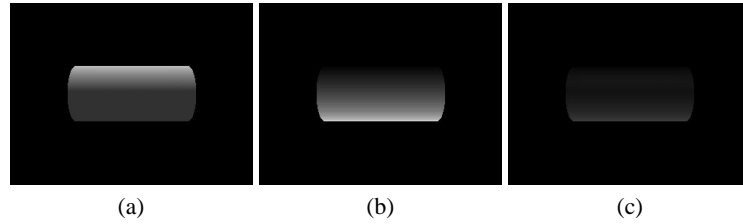


Fig. 3. Thayer’s principle of counter shading. (a) A cylinder of constant albedo under top lighting. (b) A counter-shaded cylinder under ambient lighting (produced by mapping a convex texture). (c) Thayer’s principle: the combined effect of counter-shading albedo and top lighting breaks up the shadow effect (= convex intensity function).

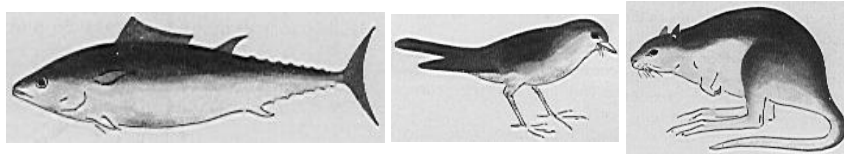


Fig. 4. Thayer’s principle. The upper part of the animal is the darker one; transition from the dark part to the bright part is obtained by a gradual change of albedo. When the animal would be in sun light, this coloration would break the convexity of the intensity function.

paint a cylinder or sphere in graded tints of gray, the darkest part facing toward the source light, and the lightest away from it, the body’s own shade so balances this color scheme that the outlines becomes dissolved. Such graded tints are typical of vertebrates and of many other animals.” Figure 3 uses ray tracing to demonstrate Thayer’s principle of counter-shading when applied to cylinders. The sketches in Fig. 4, taken from [8], demonstrate how animal coloration changes gradually from dark (the upper part) to bright (the lower part). When the animal is under top lighting (sun light), the gradual change of albedo neutralizes the convexity of the intensity function. Had no counter-shading been used, the intensity function would have been convex (as in Fig. 3(a)), exposing the animal to convexity based detectors (such as D_{arg}). Putting counter-shading into effect neutralizes the convexity of the intensity function thus disabling convexity-based detection.

The existence of counter-measures to convexity based detectors implies that there might exist predators who can use convexity based detectors similar to D_{arg} .

3.2 Thayer’s Counter-Shading Against D_{arg} -based Detection

Let us demonstrate how Thayer’s principle of counter-shading can be used to camouflage against D_{arg} -based detectors. In Fig. 5 we once again consider a synthetic cylinder; this time we operate D_{arg} on each of the images of that cylinder. As can be seen, the counter-shaded cylinder under top lighting (Fig. 5, Column C) attains much lower D_{arg} values than the smooth cylinder under the same lighting (Fig. 5, Column A). This is because counter-shading turns the intensity function from convex to (approximately) planar.

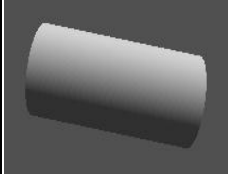
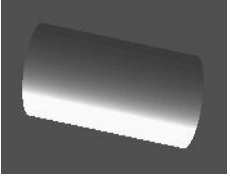
Column:	A	B	C
Texture:	Smooth.	Convex.	Convex.
Lighting:	Top.	Ambient.	Top.
Ray Tracing:			
D_{arg}^2 :			

Fig. 5. Operation of D_{arg}^2 on a counter-shaded cylinder. **Column A:** A smooth cylinder under top lighting. **Column B:** The counter-shaded cylinder under ambient lighting. **Column C:** The counter-shaded cylinder under top lighting. The counter-shaded cylinder can barely be noticed under top lighting, due to the camouflage. Under top lighting, the response of D_{arg} is much stronger when the cylinder is smooth than when it is counter-shaded, showing this type of camouflage is effective against D_{arg} .

To see the transition from a convex intensity function to a planar one due to camouflage, we draw (Fig. 6-left) the vertical cross-sections of the intensity functions of Fig. 5. The smooth cylinder under top lighting (Column A) produces a convex cross-section. The albedo, or the counter-shaded cylinder under ambient lighting (Column B), consists of graded tints of gray (i.e. convex counter-shading). Finally, the counter-shaded cylinder under top lighting (Column C) produces a flat intensity function, which means a lower probability of detection by D_{arg} .

We verify that the flat intensity function is indeed harder to detect using D_{arg} than the convex intensity function: we show that D_{arg} has a lower response to the counter-shaded cylinder under top lighting than it has to the smooth cylinder under the same lighting. This is obvious from Fig. 6-right which shows the vertical cross-sections of the responses of D_{arg} to the various images of the cylinder.

The above demonstrates that Thayer’s principle of counter-shading is an effective biological camouflage technique against convexity-based camouflage breakers, and more specifically, against D_{arg} . One can thus speculate that convexity-based camouflage breaking might also exist in nature (or else, the camouflage against it would be unnecessary).

4 Experimental Results

In this section we juxtapose the D_{arg} operator with a typical edge-based operator—the radial symmetry transform [9]—as camouflage breakers. This operator seeks generalized symmetry, and has been shown there to generalize several edge-based operators.

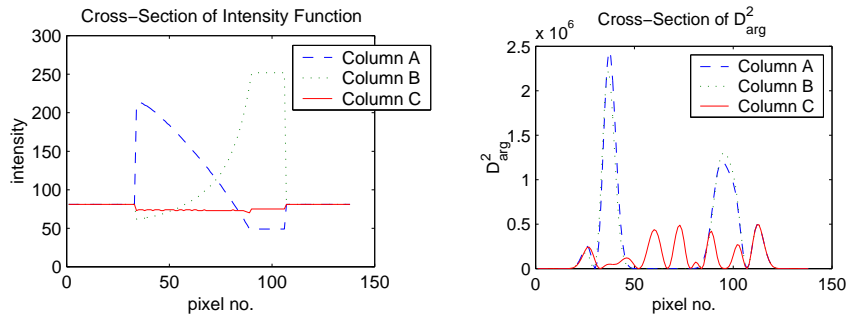


Fig. 6. Cross-sections (parallel to the y -axis, at the center of the image) of: **Left:** The intensity functions of Fig. 5. Thayer's counter-shading yields a flat intensity function for a cylinder. **Right:** D_{arg}^2 of Fig. 5. Under top lighting, the flattened intensity function of the counter-shaded cylinder has a lower D_{arg} response than that of the convex intensity function of the smooth cylinder.

We compare D_{arg} with edge-based methods, since camouflage by super-excitation of a predator's edge detectors is evident in the animal kingdom [7] (which implies edges are biologically used for camouflage breaking).

The radial symmetry operator is scale-dependent, while the peaks of D_{arg} are not. Therefore, we have compared D_{arg} with radial symmetry of radii: 10 and 30 pixels (i.e, 2 radial symmetry transformations performed for each original image). In the paper, only one radius is introduced per original, but similar results were obtained for the other radius as well.

Apatetic Coloration in Animal Animals use various types of camouflage to hide themselves, one of which is apatetic coloration. Fig. 7 exhibits a natural camouflage of a squirrel in a leafy environment under the shades of a nearby tree. The camouflaged fur has many edges which mix with the environment, preventing the radial symmetry operator from isolating any specific target. D_{arg} , however, produces a single strong peak, exactly on the squirrel. The convexity of the squirrel (and in particular, its belly) is the reason for its detection by D_{arg} . The only smooth 3D convex region in the image is the belly of the squirrel. Though some of the shades might look similar to the belly of the squirrel (even to a human viewer), they do not possess the property of being a projection of a 3D convex object, so their graylevels introduce no 3D convexity.

Another example of camouflage by apatetic coloration is Fig. 8. The figure shows two Rocky Mountain sheep (*Ovis Canadensis*) in their natural rocky environment. The coloration of the Rocky Mountain sheep fits their habitat (pay attention in particular to the upper sheep in Fig. 8). D_{arg} detects the sheep as the main subject, since they appear smooth (from the photographic distance), and are three dimensional and convex. Due to the apatetic coloring, the rocky background produces much stronger edges than the sheep, thus attracting edge-based methods. Radial symmetry specifies no single target.

Military Camouflage Breaking camouflage of concealed equipment is of particular interest. Figure 9 presents a tank in camouflage paints in front of a tree. The tree produces

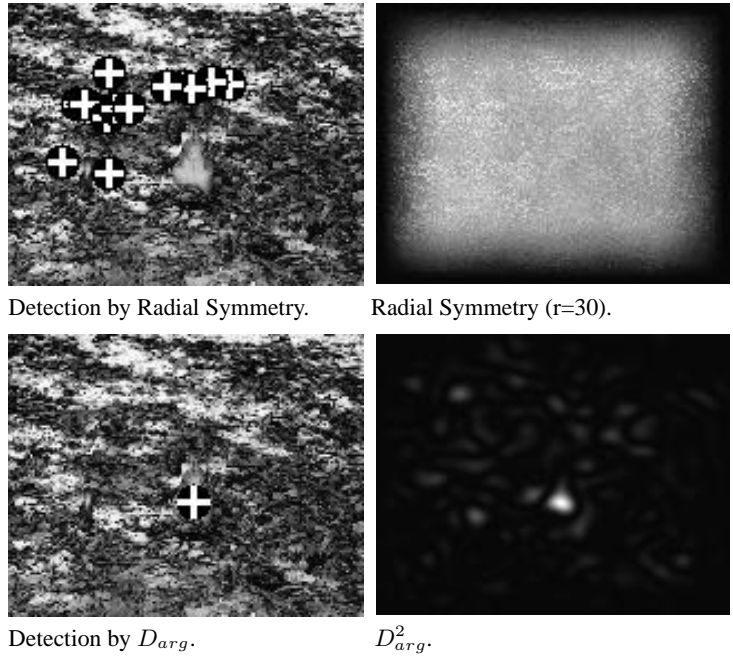


Fig. 7. A hidden squirrel. The squirrel is on a leafy ground shaded by a tree. The shades and leaves form many edges “deluding” edge-based methods. Even human viewers find it difficult to locate the squirrel in the image. D_{arg} detects the squirrel, breaking the camouflage.

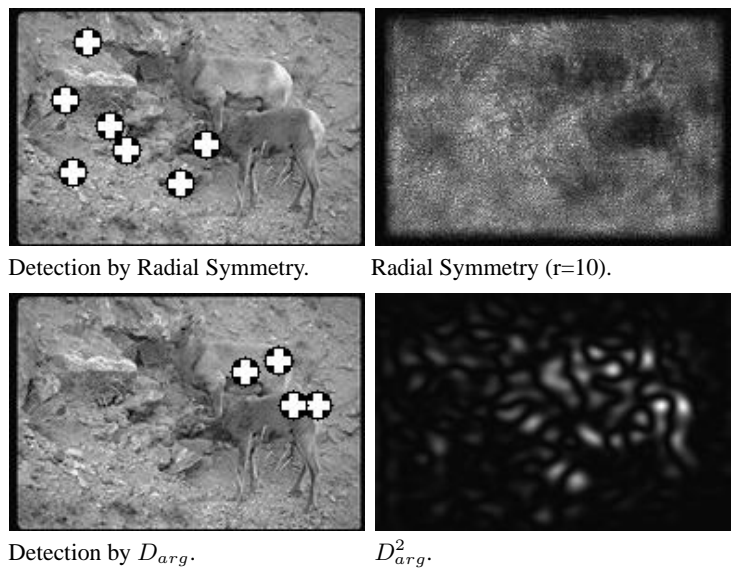


Fig. 8. Rocky mountain sheep in their rocky habitat. Edge based methods fail to detect the sheep due to its apatetic coloration. D_{arg} , however, highly responds to the convexity of the intensity function.

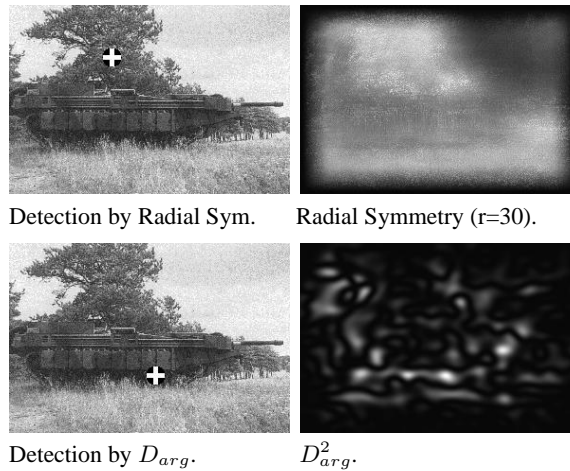


Fig. 9. A tank in camouflage paints. Convexity-based detection using D_{arg} is *not* distracted by the background (tree, grass). The tree distracts edge-based detection.

edges distracting the radial symmetry operator. The convexity of the intensity function near the wheels of the tank exposes the tank to the D_{arg} detector.

An example of breaking clothes camouflage appears in Fig. 10. Camouflage clothes on the background of dense bushes and a river makes the subject very hard to detect. Edge based detection misses the subject. D_{arg} isolates the camouflaged subject, but with one outlier (out of three detections).

5 Conclusions

Thayer's principle states that various animals use counter-shading as a major basis for camouflage. The observation of such a counter-measure in animals implies that other animals might use convexity detection to break camouflage (or otherwise there was no need for the counter-measure). We illustrate how Thayer's counter-shading prevents detection based on the convexity of the graylevel function (D_{arg}). The effectiveness of camouflage breaking by convexity detection (for subjects which are not counter-shaded according to Thayer's principle) is demonstrated using D_{arg} . The operator D_{arg} is basically intended for detection of image domains emanating from smooth convex or concave 3D objects, but the smoothness assumption can be relaxed. Finally, a comparison between the convexity-based camouflage breaker (D_{arg}) and an edge-based operator (radial symmetry) has been delineated. Convexity-based camouflage breaking was found to be highly robust and in many cases much more effective than edge-based techniques.

References

1. A. C. Copeland and M. M. Trivedi. Models and metrics for signature strength evaluation of camouflaged targets. *Proceedings of the SPIE*, 3070:194–199, 1997.

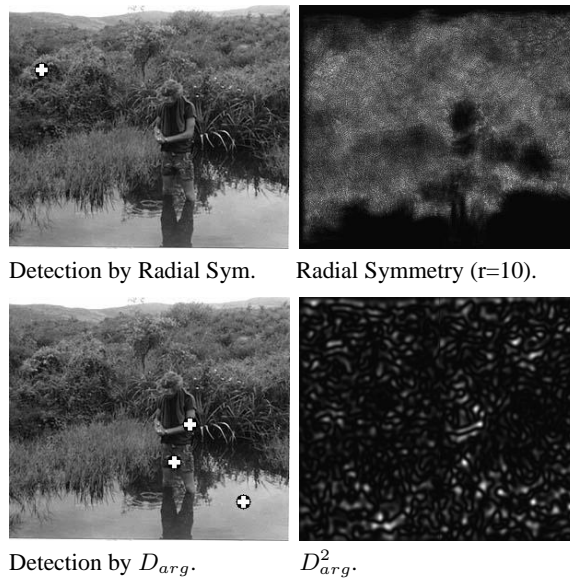


Fig. 10. A camouflaged soldier on the bank of a river near dense bushes. The edge distribution of the soldier unites with the camouflage (especially the helmet). In spite of the strong camouflage, D_{arg} detects the soldier in 2 out of 3 locations it isolates. The incorrect detection is of clouds reflecting in the water.

2. F. M. Gretzmacher, G. S. Ruppert, and S. Nyberg. Camouflage assessment considering human perception data. *Proceedings of the SPIE*, 3375:58–67, 1998.
3. Song Guilan and Tang Shunqing. Method for spectral pattern recognition of color camouflage. *Optical Engineering*, 36(6):1779–1781, June 1997.
4. Lu Huimin, Wang Xiuchun, Liu Shouzhong, Shi Meide, and Guo Aike. The possible mechanisms underlying visual anti-camouflage: a model and its real-time simulation. *IEEE Transactions on Systems, Man & Cybernetics, Part A (Systems & Humans)*, 29(3):314–318, May 1999.
5. S. Marouani, A. Huertas, and G. Medioni. Model-based aircraft recognition in perspective aerial imagery. In *Proc. of the Intl. Symposium on Comp. Vision*, pages 371–376, USA, 1995.
6. S. P. McKee, S. N. J. Watamaniuk, J. M. Harris, H. S. Smallman, and D. G. Taylor. Is stereopsis effective in breaking camouflage? *Vision Research*, 37:2047–2055, 1997.
7. D. Osorio and M. V. Srinivasan. Camouflage by edge enhancement in animal coloration patterns and its implications for visual mechanisms. *Proceedings of the Royal Society of London B*, 244:81–85, 1991.
8. Adolf Portmann. *Animal Camouflage*, pages 30–35. The University of Michigan Press, 1959.
9. Daniel Reissfeld, Haim Wolfson, and Yehezkel Yeshurun. Context free attentional operators: the generalized symmetry transform. *Intl. Journal of Computer Vision*, pages 119–130, 1995.
10. Ariel Tankus, Yehezkel Yeshurun, and Nathan Intrator. Face detection by direct convexity estimation. *Pattern Recognition Letters*, 18:913–922, 1997.
11. I. V. Ternovskiy and T. Jansson. Mapping-singularities-based motion estimation. *Proceedings of the SPIE*, 3173:317–321, 1997.
12. Abbott H. Thayer. An arraignment of the theories of mimicry and warning colours. *Popular Science Monthly, N.Y.*, pages 550–570, 1909.